# Minimum Impulse Limit Cycle Design to Compensate for Measurement Uncertainties

E.T. Kubiak*
*NASA Johnson Space Center, Houston, Texas*
and
M.W. Martin†
*Lockheed Engineering and Management Services Company, Inc., Houston, Texas*

**A new design was developed for the Space Shuttle transition phase digital autopilot to reduce the impact of large measurement uncertainties in the rate signal during attitude control. The signal source, which was dictated by early computer constraints, is characterized by large quantization, noise, bias, and transport lag that produce a measurement uncertainty larger than the minimum impulse rate change. To insure convergence to a minimum impulse limit cycle, the design employed bias and transport lag compensation and a switching logic with hysteresis, rate deadzone, and "walking" switching line. The design background, the rate measurement uncertainties, the design solution, and the performance improvement are presented in this paper.**

## Nomenclature

| | |
|---|---|
| DB | = deadband |
| $K$ | = step counter for walking switching line, $K=0,1,2,\ldots$ limit |
| $K_{\mathrm{REL}}$ | = estimated portion of jet firing not immediately seen due to lag |
| $K_{\mathrm{STEP}}$ | = step size of walking switching line |
| ROT-JET-CMD | = −1, 0, 1 jet firing command, the sign of which indicates sign of desired rotational acceleration |
| $T$ | = time between inertial measurement unit samples |
| $U_c$ | = phase-plane jet acceleration |
| $X$ | = phase-plane rate error |
| $Y$ | = phase-plane attitude error |
| $Z$ | = $Z$ transform |
| $\Delta\theta_{\mathrm{IMU}}$ | = attitude change between inertial measurement unit samplings |
| $\omega_{\mathrm{BIAS}}$ | = estimated rate gyro assembly bias |
| $\omega_{\mathrm{COMMAND}}$ | = command body rate, equal to 0 for attitude hold |
| $\omega_{\mathrm{RGA}}$ | = selected rate gyro assembly output |
| $\omega_{\mathrm{RGA\text{-}CORRECTED}}$ | = rate gyro assembly output with corrections |

## Background

DURING flight of the Space Shuttle, three separate onboard computer loads, referred to as the ascent, on-orbit, and entry computer loads, in accordance with their respective mission phases, are used to provide control. The transition phase digital autopilot (Trans DAP) resides within both ascent and entry computer loads and performs the necessary control functions encountered during the exoatmospheric part of the late ascent and early entry phases. Using the primary reaction control system (PRCS) jets and the orbital maneuvering system (OMS) as control effectors, the Trans DAP provides attitude control during external tank separation through orbit circularization on ascent and during deorbit on entry. Due to the complex nature of the ascent and entry flight regimes, both the ascent and entry computer loads were near capacity in memory and CPU utilization at the time of the initial design. Hence, an early Trans DAP design requirement was to minimize the use of memory and CPU consistent with acceptable performance characteristics. This requirement implicitly forced the selection of the rate gyro assemblies (RGA) as the source of rate information since the RGA information was the only sensor data available at the autopilot's execution frequency, 12.5 Hz.

However, the process of reading the RGAs added significant uncertainty to the rate information. The presence of large quantization, noise, and bias, coupled with transport lag, conspired to produce an uncertainty in the rate signal significantly larger than the minimum impulse rate change provided by the PRCS. The original design did not compensate for these uncertainties and, upon inclusion of the measurement uncertainties into simulations, PRCS usage rose by as much as twentyfold. At a small cost to memory and CPU, design modifications were developed that compensated for the quality of the rate sensor data. This compensation in the attitude control loop is the subject of this paper.

## Rate Measurement Uncertainties

There are two principal sources of the uncertainties introduced into the RGA signal, the analog/digital (A/D) conversion process and transport lag. The A/D conversion occurs in the Orbiter's multiplexer demultiplexer (MDM), which is the standard interface between the Orbiter's onboard computers and its sensors/effectors. This process causes large measurement errors in the form of quantization, noise, and bias to be induced into the signal. Even though the RGAs are accurate to 0.01 deg/s, the signal is quantized to 0.08 deg/s in roll and 0.04 deg/s in pitch and yaw. These large quantization values are the result of scaling for the worst-case rates expected during ascent and entry, ±40 deg/s in roll and ±20 deg/s in pitch and yaw, which are far in excess of the needs of an orbit autopilot. Figure 1 outlines the resulting noise distribution and bias from test results of the MDM quantization process. Each noise count represents one MDM quantization level. The noise on the signal has a near Gaussian distribution with a standard deviation of approximately 0.6 of a quantization level. From Fig. 1, it is seen that for a 99% confidence level in the measurement the un-

---

Presented as Paper 82-1578 at the AIAA Guidance and Control, Atmospheric Flight Mechanics, and Astrodynamics Conference, San Diego, Calif., Aug. 9-11, 1982; submitted Aug. 27, 1982; revision received April 19, 1983. 

*Project Engineer
†Engineer. Member AIAA.

certainty due to noise is three quantization levels. The bias is seen to be approximately $-0.4$ quantization levels.

The other source of measurement uncertainty arises from transport delays and hardware response times. The relative phasing of events, RGA sampling, autopilot execution, and jets fired, combined with the inherent delays in software and hardware, can result in the RGA sensing less than half of the previous cycle's rate change due to a command thruster firing. Figure 2 illustrates the sequence of events and portions of the impulse sensed by the RGA. As depicted, the Trans DAP executes every 80 ms and a minimum impulse jet firing is of the same duration. The lag between RGA sampling and DAP execution is 18 ms. Finally, the lag between the DAP commanding a jet on and full thrust is approximately 32 ms and the jet-off delay is approximately 23 ms. Hence, the total transport lag between RGA sampling and full thrust is some 50 ms and the RGA "sees" only a portion, 30 ms, of a jet firing commanded by the DAP on the previous pass. It is not until one full DAP cycle later that the full rate change due to a minimum impulse jet firing can be sent to the DAP.

## Impact of Rate Measurement Uncertainties

Typical PRCS minimum impulse rate changes are approximately 0.057 deg/s for roll, 0.074 deg/s and 0.05 deg/s for positive and negative pitch, respectively, and 0.040 deg/s for yaw. However, the measurement uncertainty, which is approximately three quantization levels, or 0.24 deg/s in roll and 0.12 deg/s in pitch and yaw, is a factor of two to four times the minimum impulse rate change. Rate time histories of actual and sensed rates are given in Fig. 3. This figure illustrates how the measurement uncertainties dominate the rate signal during attitude control.

Since these rate signal uncertainties are much larger than the PRCS minimum impulse rate change, considerable undershooting and overshooting in attitude rate control can occur. Undershooting causes excessive PRCS pulsing with a corresponding reduction in thruster mission lifetime and inefficient propellant usage due to inexact synchronization of openings and closings of fuel and oxidizer valves. Shuttle flight crews have commented on the howitzer-like sound that the PRCS makes when fired, thus from a human-factors standpoint, excessive pulsing is undesirable. Excessive pulsing may also cause structural problems on future flights with more flexible payloads. Further, for a double-sided limit cycle, overshooting causes excessive limit cycle rates and an increase in propellant usage proportional to the square of the ratio of the actual to minimum firing times. Thus, a limit cycle of twice the minimum impulse limit cycle will use four times as much propellant since the DAP must fire twice as long twice as often. Efficient propellant usage is a requirement for Shuttle operations and thus minimization of undershoot and overshoot is a necessity.

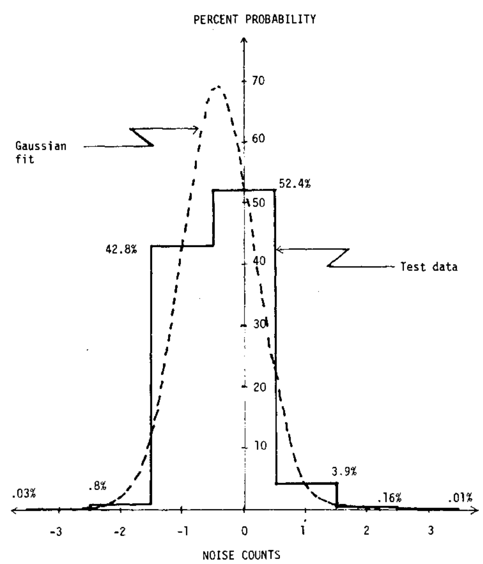


**Fig. 1 MDM noise test results from Ref. 1 (mean = $-0.4016$, standard deviation = 0.5892).**

## Design Solution

The design solution developed to insure convergence to a minimum impulse limit cycle employed multiple techniques easily adapted to the Trans DAP attitude control loop. RGA selection filtering, bias and transport lag compensation, a rate deadzone, and a "walking" switching line were added to minimize the impact of the large rate measurement uncertainties. The selection filtering, bias compensation, and transport lag compensation reduce overall measurement errors. The remaining changes are modifications to the phase-plane switching logic and desensitizing the autopilot to the remaining measurement uncertainties.[2] It should be noted that the original phase-plane switching logic was similar to those that flew quite successfully in Apollo; however, they were not, of course, designed to accept the Shuttle-type measurement uncertainty.[3,4]

The RGA selection filtering and bias compensation are in Trans DAP support routines and reduce the overall effective rate uncertainty. The first algorithm, the RGA selection filter, runs at the DAP cycle rate (12.5 Hz) and operates on the MDM-supplied RGA outputs. For each axis it determines the rate output $\omega_{RGA}$ as the midvalue reading from three independent RGAs. The other algorithm performs rate bias correction via attitude data from the inertial measurement unit (IMU) and operates at 1.04 Hz. The estimated bias, $\omega_{BIAS}$, is subtracted from $\omega_{RGA}$ and this new rate, $\omega_{RGA\text{-}CORRECTED}$, is sent to the DAP,

$$\omega_{RGA\text{-}CORRECTED} = \omega_{RGA} - \omega_{BIAS}$$

$\omega_{BIAS}$ is computed by first comparing the IMU-measured body angle change with the body angle change predicted by

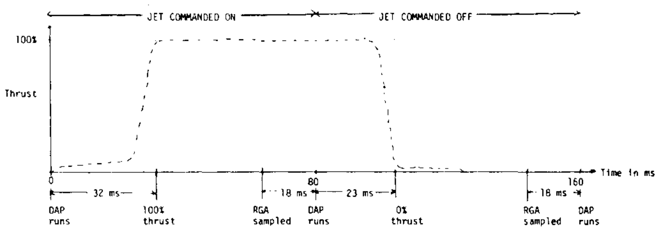


**Fig. 2 Transport delays (DAP turns jet on at 0 ms and off at 80 ms).**

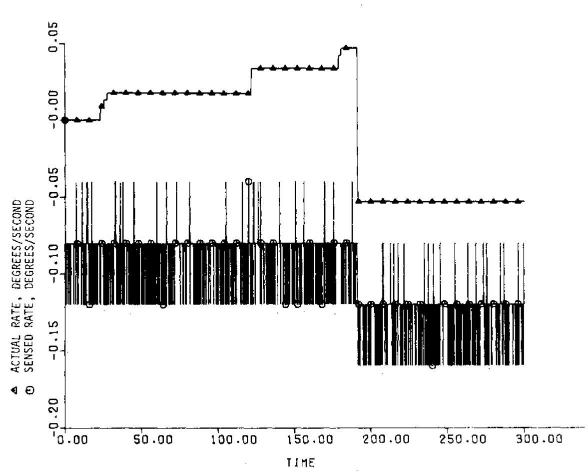


**Fig. 3 Actual rate and sensed pitch rate vs time.**

the $\omega_{\text{RGA-CORRECTED}}$ extrapolation,

$$\Delta\theta = \Delta\theta_{\text{IMU}} - T\frac{1+Z^{-1}}{2}\,\omega_{\text{RGA-CORRECTED}}$$

Then $\omega_{\text{BIAS}}$ is computed as:

$$\omega_{\text{BIAS}} = Z^{-1}\omega_{\text{BIAS}} + 0.1 \times (\Delta\theta / T)$$

The net effect of the first algorithm is to reduce the probability of large noise spikes (two or three quantization levels) being passed through to the DAP. It also culls output readings of an individual MDM/RGA combination with a large bias. The second algorithm tends to reduce bias due to both MDM noise and the quantization process itself, particularly for slowly changing rates.

Lag due to hardware and software synchronization is compensated for by adding a predictive rate increment to the $\omega_{\text{RGA-CORRECTED}}$ on a per-axis basis,

$$\omega_{\text{RGA-CORRECTED}} = \omega_{\text{RGA-CORRECTED}} + \text{ROT-JET-CMD} \times K_{\text{REL}}$$

In the above equation, ROT-JET-CMD is sign of the prior cycle's thruster command $(-1,0,+1)$ and $K_{\text{REL}}$ is the estimated magnitude of the prior cycle's rate change not yet measured because of the delays. Hence $K_{\text{REL}}$ is an approximation of thruster control acceleration times the delay time.

The rate input to the Trans DAP, $\omega_{\text{RGA-CORRECTED}}$, nonetheless, still contains significant jitter (up to one or more quantization values) and a special switching logic was designed to cope with the problem. To explain how the switching logic works, it is instructive to examine the state trajectory shown in Fig. 4. The trajectory indicates the desired convergence to a minimum impulse limit cycle. Beginning in the rate limit coast zone (point A) the state drifts to the "primary" switching curve (point B). Here the desired control action is to drive the rate to zero in one continuous firing. To this end the "slope" of the switching curve is made slightly more shallow than that of the trajectory from the control firing by the inclusion of a constant (1.25) in the parabolic switching curve: $x = y^2/(2\times 1.25 \times U_c) + \text{DB}$. Additionally, hysteresis is employed such that the firing will continue in the coast zone until zero rate error occurs. However, to insure that quantization jitter of $\omega_{\text{RGA-CORRECTED}}$ does not cause overfiring, the rate error is set to zero if its magnitude is less than or equal to a quantization level. Therefore, upon termination of the rate damping firing (point C), there will likely be some residual rate—typically less than a minimum impulse—change and the state will drift to the primary switching line (point D). Here the sign of the rate must be reversed, but for minimum impulse limit cycle convergence the resulting rate must be no further past zero than a minimum impulse rate change.

As the rate uncertainty is actually larger than a minimum impulse rate change, rate information alone cannot accurately detect rate reversal. An attitude hysteresis scheme is employed to determine the rate reversal. Figure 5, a blowup of Fig. 4 about point D, illustrates the principle of the hysteresis. At point D a minimum impulse control firing is commanded and rate reversal may have occurred. But even if it has occurred, on succeeding DAP cycles rate jitter may cause another crossing of the switching curve, producing an extra firing. This is avoided by shifting or "walking" the primary switching line to the right by a small attitude increment each time a control firing is initiated (up to 1.2 times the deadband). Thus the curve becomes: $x = y^2/(2\times 1.25 \times U_c) + \text{DB}(1.0 + K \times K_{\text{STEP}})$. The curve is reset to its original position $(K=0)$ when rate reversal is confirmed by the attitude error moving to a value less than 0.9 times the deadband. The state will then move toward the opposite deadband where the process is repeated and a minimum impulse limit cycle has been achieved.

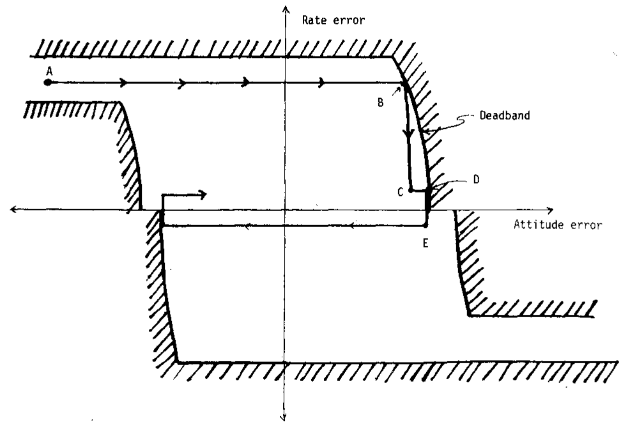


Fig. 4 Phase-plane trajectory.

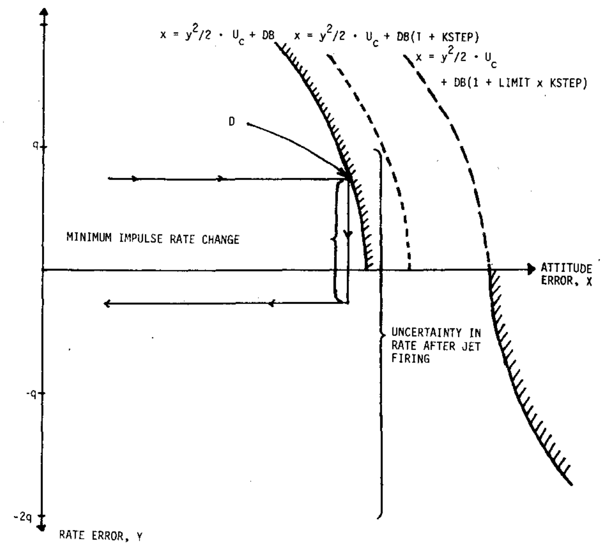


Fig. 5 Blowup of phase-plane trajectory about point D of Fig. 4 ($q$ is the quantization level).

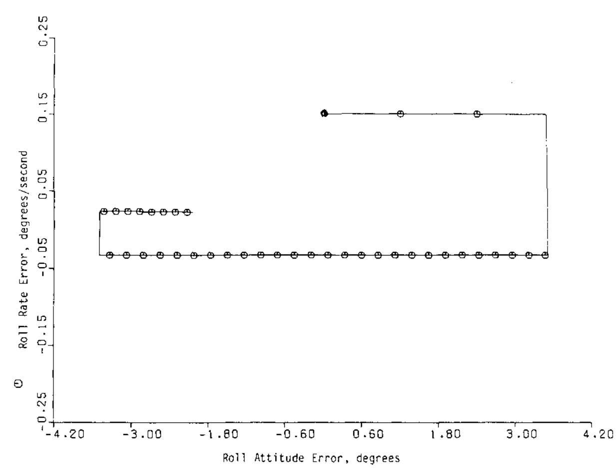


Fig. 6 Phase plane from test case 1, ideal rate sensor, no measurement uncertainties.

## Performance Improvement

To illustrate the performance improvement with this new design approach, three simulation runs were made with identical run scenarios. Each run began with a roll angular rate of 0.15 deg/s and ran for 300 s to test for limit cycle convergence. The results of the first run are illustrated in Fig. 6 and demonstrate convergence with the original design if there were no measurement uncertainties (ideal rate sensor).

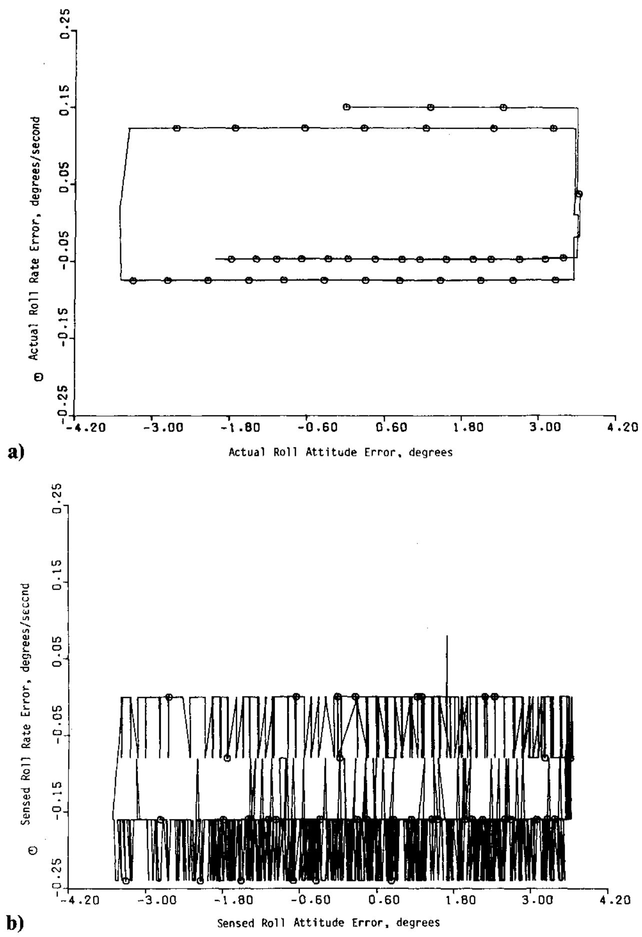


**Fig. 7 Phase plane from test case 2, measurement uncertainties included: a) actual trajecory; b) sensed trajectory.**

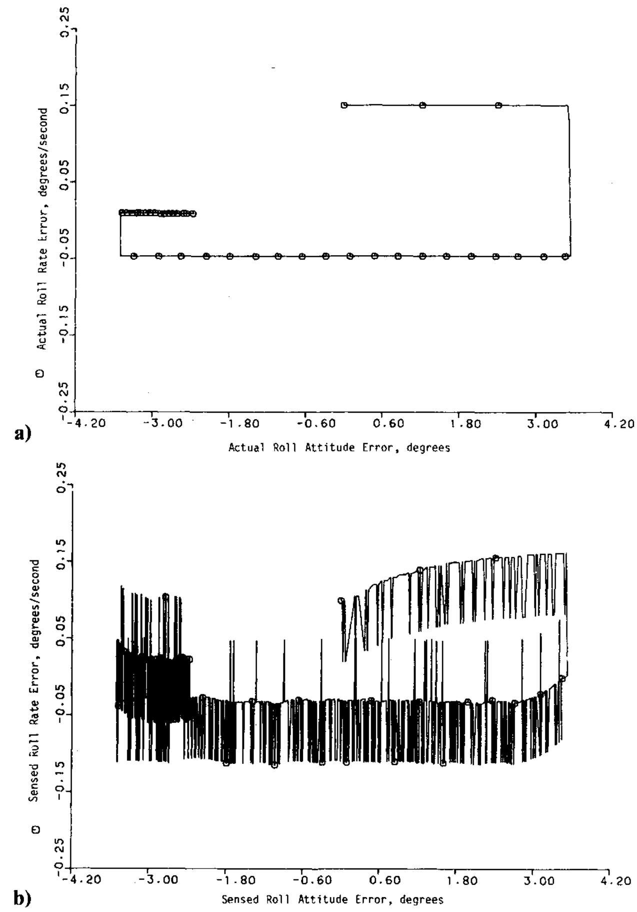


**Fig. 8 Phase plane from test case 3, measurement uncertainties and new design included: a) actual trajectory; b) sensed trajectory.**

The results of the second run, shown in Fig. 7, depict the same initial conditions, but with the measurement uncertainties added. Figure 7a is the actual phase-plane trajectory, while Fig. 7b is the sensed trajectory. Finally, the last run included both the measurement uncertainties and the new design. Results are shown in Fig. 8, with Fig. 8a being the true trajectory and Fig. 8b the sensed trajectory.

From the phase-plane trajectories of the figures, it is apparent that minimum impulse limit cycle convergence is surrendered when the measurement uncertainties are coupled with the original design, Fig. 6 vs Fig. 7a. Equally apparent from Fig. 8a, the design update regained minimum impulse limit cycle convergence. Performance for the first and third runs was nearly identical, whereas comparatively, the net thruster firing time for the second run was approximately twice as long. Extended time duration runs have indicated similar trends. Performance of the updated design with or without the inclusion of the measurement uncertainties closely approaches the ideal limits, whereas minimum impulse cycle convergence is not achievable with the original design when the measurement uncertainties are included.

## Summary

The foregoing has documented a new design approach for coasting flight rotational control to achieve a minimum impulse limit cycle in the presence of significant measurement uncertainties (quantization, noise, bias, and transport lag). This approach differed considerably from more traditional methods such as used in Apollo, where its primary controller used IMU filtering to derive the rate and its backup controller used filtered RGA data. Neither of these approaches was applicable. A derived-rate implementation was not viable because the IMU could not be sampled more often than 1.04 Hz and also its feed-forward logic may have exceeded the then-available computer memory. Filtering of the RGA output was unacceptable because the filter bandwidth requirement would imply a significant net increase in the already large effector-to-sensor lag. Hence, a new design approach was defined that employed multiple compensations to reduce rate data uncertainties and a phase-plane logic to desensitize itself to remaining rate data uncertainties. Integration of this design concept with a digital phase-plane-type controller entails only a small increase in computer memory and processing. Further, the approach was employed in the Orbiter flight control mechanization, and both simulation and flight data have verified that its performance is comparable to that expected with an ideal rate sensor.


## Acknowledgments

The authors wish to recognize the efforts of R.L. Stuva at the Charles Stark Draper Laboratory and others at both CSDL and Rockwell International for their contributions which led to the incorporation of this concept in the Space Shuttle flight control design.


## References


[1]Rockwell International, Internal letter 383-250-WDD-078-003, Feb. 20, 1978.

[2]"Space Shuttle Orbital Flight Test, Level C Functional Subsystem Software Requirements," Rockwell International, Rept. SD 76-SH-0008, Vol. 2.

[3]Peters, W.H. and Cox, K.J., "Apollo Experience Report: Guidance and Control Systems – Digital Autopilot Design Development," NASA TN D-7289, June 1973.

[4]Cherry, G.W., "Design Principles for an Integrated Guidance and Control System for the Lunar Excursion Module," *AIAA Manned Space Flight Meeting*, AIAA A66-1161303-05, Oct. 1965, pp. 145-157.